

# Comparative Analysis of Models for Fischer-Tropsch Synthesis in Slurry Reactors

M. K. Oduola and M. Iriwogu

koyejo.oduola@uniport.edu.ng

Department of Chemical Engineering, University of Port Harcourt, Nigeria

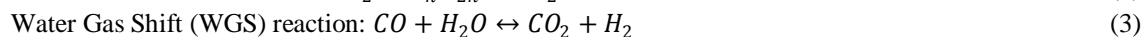
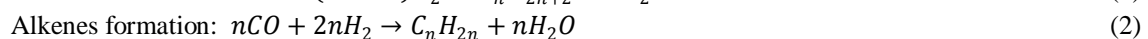
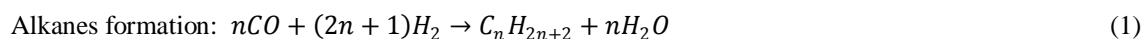
**ABSTRACT :** *Two approaches identified in literature for modeling slurry bubble column reactors for Fischer-Tropsch synthesis is presented and compared in this work. The first approach, Uniform Bubble Model (UBM) assumes the gas bubbles moving up the reactor are of uniform sizes, while the second model termed Large-Small Bubble model (LSBM) takes cognizance of the presence of large and small bubbles. It is assumed that both the gas and liquid phases are axially dispersed. Reaction and hydrodynamic parameters are estimated and the sets of equations obtained are solved using MATLAB pdepe solver for hydrogen gas conversion. Results obtained for a typical industrial scale reactor (30m long, 8m in diameter, gas entering at 0.35m/s and 35 vol% catalyst load) indicates that the models (UBM and LSBM) can adequately predict the reactor's performance for gas conversion. The UBM predictions were persistently greater than the LSBM values. Different equations for gas holdup were incorporated in the models and compared for various reactor constraints. The results revealed that the disparity in the models prediction may be related to the method used in deriving the gas holdup value. The results also showed that taller reactors, higher catalyst loadings and lower gas velocity leads to improved conversion.*

**KEYWORDS – Fischer-Tropsch reaction, Gas-to-Liquid, Gas bubble sizes, Mass transfer, Slurry reactors**

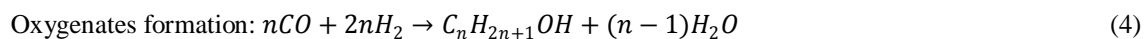
## 1. Introduction

The Gas-to-Liquid (GTL) process involves methods and technologies used in converting natural gas and other gaseous hydrocarbons into liquid hydrocarbon products for easy transportation. This chemical conversion process yields cleaner burning products such as naphtha, transportation fuels, lubricants and other chemicals such as methanol [1, 2]. This conversion can be achieved using the Fischer-Tropsch synthesis – a highly exothermic reaction where synthesis gas (a mixture of hydrogen and carbon (II) oxide) is reacted in the presence of solid catalysts to produce liquid hydrocarbons. The Fischer-Tropsch (F-T) synthesis is a polymerization process that yields mainly linear alkanes and alkenes as well as oxygenated organic products. The hydrocarbons produced are refined and upgraded using standard refining and reforming methods. The F-T reactions taking place are as follows [2, 3];

- Main reactions:



- Side reactions:



Where n represents the number of carbon atoms.

The prevailing reaction depends on the feed gas ratio ( $\text{H}_2/\text{CO}$ ), the type of catalyst used, reactor type and process conditions [1, 2]. In commercial plants, the process conditions and catalyst are carefully chosen to favour the production of middle distillate hydrocarbons and diesel fuel fractions and produce less of other products like methane [4, 5].

Slurry bubble column reactors (SBCR) in recent years have garnered great research interest for use in several industrial processes including the Fischer-Tropsch conversion of synthesis gas to liquid fuels. SBCRs are multiphase flow reactors where the inlet gas is bubbled through slurry (liquid and solid catalyst mixture). For the Fischer-Tropsch

reaction this slurry consist of finely divided catalysts (usually cobalt or iron) distributed in the complex liquid wax produced by the process [1, 6]. The synthesis gas reacts in contact with the catalyst in the slurry to produce the products. The advantages of using this reactor include- better temperature control and heat removal as well as ease of construction.

Proper design and scale up of SBCR is necessary for improved productivity and profitability and a great deal of analysis and study has been done to design, simulate, scale-up and investigate its hydrodynamics. In modeling the SBCR, two broad approaches are recognized in literature – models based on gas bubbles of uniform sizes and more recently the two bubble class in the gas phase. Van der Laan [7] gave a précis of popular models used for modeling the SBCR. A good number of these models, described the flow pattern as plug flow, completely mixed, dispersed plug flow or combined two or more of these approaches to model the gas and liquid (slurry) flow in the reacting vessel. The solid catalyst particles are usually very small in size (less than 50 $\mu$ m) consequently, the solid suspension in some of the published works reviewed was considered a pseudo-homogeneous slurry phase. However, some models like those of Prakash and Bendale [8], Sehabiague et al. [9] used the sedimentation dispersion model to account for axial concentration of the solids.

The gas is usually modeled as a single phase (i.e. consist of evenly sized bubbles), but industrial F-T reactors are reported to operate in the heterogeneous regime [10, 11]. In this heterogeneous mode, bubbles of varying sizes exist and are broadly divided into two classes - large and small bubbles. Inga [12] reviewed some of the earlier slurry reactor models for F-T synthesis. These early models considered the gas phase to consist of bubbles of uniform sizes that was either completely mixed, in ideal plug flow or dispersed plug flow. This assumption of uniform gas bubbles has been implemented in a number of literatures [8, 13, 14, 15] to describe the flow pattern of the gaseous reactants.

For commercial slurry reactors operated in the heterogeneous regime, modifications were made to the early models to account for bubbles of different sizes in the gas phase. In this new approach the gas phase is modeled assuming gas bubbles of two broad classes – Large and small bubbles. Several researchers [7, 9, 16, 17, 18] used the large-small bubble concept to develop SBCR models. Rados et al. [17] and Iliuta et al. [19] pointed out that the assumption that only bubbles of uniform sizes are present, may cause an exaggeration of gas conversion level if gas-liquid mass transfer is controlling. Mareto and Krishna [16], Van der Laan et al. [20] and Wang et al. [18] developed their model equations considering the presence of large and small gas bubbles. The flow of the larger bubbles was modeled assuming plug flow, while the smaller bubbles and liquid were modeled as completely mixed. Van der Laan et al. [20] unlike the others mentioned used kinetics for an iron catalyst and describe the products selectivity using the  $\alpha$ -olefin readsorption product distribution model [7]. The various researchers used their models to simulate reactors imposed with typical industrial scale constraints. Sehabiague et al. [9], De Swart and Krishna [21] described the gas flow pattern (both large and small bubbles) and liquid phases using the dispersed plug flow model. While the former used Yates and Satterfield [22] kinetic rate equation, the latter used a simple first order kinetic rate equation in terms of hydrogen. Hooshyar et al. [23] did a comparison of the single and two-bubbles modeling approach for SBCR and concluded that there is no significant difference between the two approaches in terms of temperature, concentration and conversion profile. Papari et al. [24] modeled Dimethyl Ether (DME) synthesis in slurry bubble reactors and posited that the large-small bubble approach gave results that were closer to experimental results.

The objective of this work is to develop mathematical models for SBCR for Fischer-Tropsch synthesis on the basis of uniform (single) and two (large and small) bubble classes in the gas phase and compare their predictions for gas concentration and conversion profile. A systematic comparison is carried out to investigate the resourcefulness and sensitivity of the different approach in predicting reactor performance when reactor geometry and operating variables are changed. In the design, modeling and scale-up of SBCR the coefficients describing the transfer of materials and the hydrodynamics are important parameters [25, 26]. Therefore, the influence of the choice of gas holdup equations on the gas conversion predictions of the models is investigated.

## 2. Modeling Technique and Analysis

The numerical depiction of the design model of an industrial slurry bubble column reactor for the Fischer-Tropsch process is presented in this section. Two reactor models are put-forward. Model 1 is built on the idea of the single-sized bubbles in the bubbly regime termed Uniform Bubble Model (UBM) for this enquiry while Model 2 which assumes two gas bubble classes is termed the Large-Small Bubble Model (LSBM). The models are material balances of the gas and liquid phases. In slurry reactors the gas is supplied to the bottom of the reactor and is sparged using

distributors. These models are based on the following assumptions:

- Both the gas and slurry (liquid) phase moves in dispersed plug flow. The degree of mixing of the phases in the axial direction is described using a dispersion parameter.
- Reactor operates isothermally ( $\Delta T=0$ ).
- Uniform catalyst distribution.
- Catalyst effectiveness factor is one ( $\xi=1$ ).
- The resistance to the transfer of materials and heat between catalyst and liquid are negligible due to small catalyst particle sizes.
- The resistance to the transfer of materials in the bulk gas phase and liquid-solid inter-phase are negligible when compared with that of the bulk liquid.
- Inert liquid phase.

The gas velocity changes as it moves up the reactor due to chemical reaction. This reduction in the gas speed is taken care of using the linear relationship credited to Levenspiel [7, 16, 27]. It is expressed as a function of syngas conversion as specified in Equation 6:

$$U_g = U_{go} (1 + \alpha_c X_{CO+H_2}) \quad (6)$$

And

$$X_{CO+H_2} = \left( \frac{1+U}{1+F} \right) X_{H_2} \quad (7)$$

$U_{go}$  (m/s) represents the inlet/feed gas velocity,  $\alpha_c$  the gas contraction factor,  $X_{CO+H_2}$  and  $X_{H_2}$  are syngas and hydrogen conversion respectively.  $F$  is the inlet gas ratio of  $H_2$  to  $CO$ , while  $U$  is the consumption ratio of  $H_2$  to  $CO$  ( $-r_{H_2}/-r_{CO}$ ). The contraction factor can vary from -0.5 to -0.68 [16, 27]. Here,  $\alpha_c = -0.5$  is used.

## 2.1 Uniform Bubble Model (UBM)

The gas phase consists of bubbles of uniform sizes. The dimensionless form of the model equations for the gas and liquid/slurry phase is given as follows:

Gas Phase:

$$\varepsilon_g \frac{\partial y_A}{\partial \tau} = \frac{1}{Pe_g} \frac{\partial^2 y_A}{\partial z^2} - u_g \frac{\partial y_A}{\partial z} - St_g (y_A - x_A) \quad (8)$$

$$\varepsilon_L \frac{\partial x_A}{\partial \tau} = \frac{1}{Pe_L} \frac{\partial^2 x_A}{\partial z^2} - u_L \frac{\partial x_A}{\partial z} + St_L (y_A - x_A) - \frac{\varepsilon_L \varepsilon_S \rho_s L}{C_{Ai}} (-r'_A) \quad (9)$$

Where;

$$y_A = \frac{C_{A,g}}{C_{Ai}}; x_A = \frac{C_{A,L}}{C_{Ai}}; Z = \frac{z}{L}; \tau = \frac{t U_{go}}{L}$$

$$St_g = \text{Stanton number for gas} = \frac{K_L a L}{U_{go} m_A}; St_L = \text{Stanton number for liquid} = \frac{K_L a L}{U_{go}}$$

$$Pe_g = \text{Peclet number in the gas phase} = \frac{U_{go} L}{\varepsilon_g D_g}; Pe_L = \text{Peclet number in the liquid phase} = \frac{U_L L}{\varepsilon_L D_L}$$

$L$  is the reactor length (m),  $C_{Ai}$  is inlet gas concentration ( $\text{mol/m}^3$ ) and  $m_A$  is the dimensionless Henry's constant for component A

Initial conditions:

$$\text{At } \tau = 0, y_A = x_A = 0 \quad (10)$$

Boundary conditions:

Gas Phase

$$y_A = y_{Ao} = 1 \text{ at } Z = 0 \quad (11)$$

Liquid Phase

$$\frac{dx_A}{dZ} = Pe_L x_A \text{ at } Z = 0 \quad (12)$$

$$\frac{dx_A}{dZ} = 0 \text{ at } Z = 1 \quad (13)$$

## 2.2 Large-Small Bubble Model (LSBM)

The equations of the LSBM are derived by revising Equations 8 and 9 to accommodate the existence of small and large gas bubbles rising up the reacting vessel. The dimensionless forms of the LSBM equations are presented below:

Large Bubbles in the Gas Phase

$$\epsilon_B \frac{\partial y_{A,large}}{\partial \tau} = \frac{1}{Pe_{g,large}} \frac{\partial^2 y_{A,large}}{\partial Z^2} - u_B \frac{\partial y_{A,large}}{\partial Z} - St_{g,large} (y_{A,large} - x_A) \quad (14)$$

Where the subscripts 'large' represent parameters for large bubbles and  $U_B$  is the superficial gas velocity through the large bubbles given as  $U_B = U_g - U_{df}$ .

$U_{df}$  is the superficial gas velocity through the small bubbles.  $u_B$  is dimensionless gas velocity of the large bubbles. Plug flow character can be specified by setting the Peclet number for the large bubbles at a value of 100.

Small Bubbles in the Gas Phase

$$\epsilon_{df} \frac{\partial y_{A,small}}{\partial \tau} = \frac{1}{Pe_{g,small}} \frac{\partial^2 y_{A,small}}{\partial Z^2} - u_{df} \frac{\partial y_{A,small}}{\partial Z} - St_{g,small} (y_{A,small} - x_A) \quad (15)$$

The subscripts 'small' represents parameters for small bubbles, while  $u_{df}$  is the dimensionless gas velocity of the small bubbles.

Liquid Phase

$$\epsilon_L \frac{\partial x_A}{\partial \tau} = \frac{1}{Pe_L} \frac{\partial^2 x_A}{\partial z^2} - u_L \frac{\partial x_A}{\partial z} + St_{L,large} (y_{A,large} - x_A) + St_{L,small} (y_{A,small} - x_A) - \frac{\epsilon_L \epsilon_{SP} \rho_s L}{C_{Ai}} (-r'_A) \quad (16)$$

Initial Conditions:

$$\text{At } \tau = 0, y_{A,large} = y_{A,small} = x_A = 0 \quad (17)$$

Boundary Conditions:

Gas Phase (Large Bubbles)

$$y_{A,large} = y_{A0} = 1 \text{ at } Z = 0 \quad (18)$$

Gas Phase (Small bubbles)

$$\frac{dy_{A,small}}{dZ} = Pe_g (y_{A,small} - y_{A0}) \text{ at } Z = 0 \quad (19)$$

$$\frac{dy_{A,small}}{dZ} = 0 \text{ at } Z = 1 \quad (20)$$

Liquid phase

$$\frac{dx_A}{dZ} = Pe_L x_A \text{ at } Z = 0 \quad (21)$$

$$\frac{dx_A}{dZ} = 0 \text{ at } Z = 1 \quad (22)$$

### 2.3 Hydrodynamic Parameters

- Gas Holdup

The total gas holdup is estimated using equation 23 [16, 28, 29].

$$\varepsilon_g = \varepsilon_B + \varepsilon_{df}(1 - \varepsilon_B) \quad (23)$$

$\varepsilon_B$  and  $\varepsilon_{df}$  are the gas holdups for large and small bubbles respectively and are estimated using the equations below;

$$\varepsilon_{df} = \varepsilon_{df,ref} \left( 1 - \frac{0.7}{\varepsilon_{df,ref}} \cdot \varepsilon_s \right) \quad (24)$$

$$\varepsilon_B = 0.3 \frac{1}{D_c^{0.18}} \frac{1}{(U - U_{df})^{0.22}} (U - U_{df})^{4/5} \quad (25)$$

$D_c$  represents the reactor's internal diameter and is set as 1 in Equation 25. This is based on the assumption that the influence of diameter on the holdup of the large bubbles persists up to 1m [16].

The superficial gas velocity through the small bubbles  $U_{df}$  is determined using the relationship below;

$$U_{df} = \varepsilon_{df} \cdot V_{small} \quad (26)$$

The rise velocity of the small bubbles,  $V_{small}$  is given as;

$$V_{small} = V_{small,ref} \left( 1 + \frac{0.8}{V_{small,ref}} \cdot \varepsilon_s \right) \quad (27)$$

The properties of the liquid influences  $\varepsilon_{df,ref}$  and  $V_{small,ref}$  and they are obtained from experiments. The values ( $\varepsilon_{df,ref} = 0.27$  and  $V_{small,ref} = 0.095\text{m/s}$ ) used by Krishna and Sie [28] for paraffin oil is adopted. For the UBM, the overall gas holdup is obtained using Equation 23.

Simulations are also done using the gas holdup correlations given by De Swart and Krishna [21] and the Wilkinson methods [30] respectively. De Swart [31] gave the following correlations for the gas holdup at the transition point from homogeneous to heterogeneous regime as follows;

$$\varepsilon_{trans} = 2.16 \exp(-13.1 \rho_g^{-0.10} \mu_L^{0.16} \sigma^{0.11}) \exp(-5.86 \varepsilon_s) \quad (28)$$

The gas holdup calculated using Equation 28 is taken as the holdup value for small bubbles. At this point of transition, the superficial gas velocity (velocity of small gas bubbles) is obtained using Equation 29;

$$U_{trans} = V_{small} \varepsilon_{trans} \quad (29)$$

De Swart et al. [21] used Equations 28 and 29 in estimating the holdup and small gas bubbles velocity respectively. They obtained the rise velocity of the small bubbles following the Wilkinson approach [30] and used the Maretti and Krishna [16] equation to calculate the gas holdup of the large bubbles.

$$\varepsilon_g = \frac{U_{trans}}{U_{b-small}} + \frac{U_g - U_{trans}}{U_{b-large}} \quad (30)$$

$$U_{b-small} = 2.25 \frac{\sigma_L}{\mu_L} \left( \frac{\sigma_L^3 \rho_L}{\mu_L^4 g} \right)^{-0.273} \left( \frac{\rho_L}{\rho_g} \right)^{0.03} \quad (31)$$

$$U_{b-large} = U_{b-small} + 2.4 \frac{\sigma_L}{\mu_L} \left( \frac{\mu_L (U_g - U_{trans})}{\sigma_L} \right)^{0.757} \left( \frac{\sigma_L^3 \rho_L}{\mu_L^4 g} \right)^{-0.077} \quad (32)$$

$$U_{trans} = 0.5 \times U_{b-small} \exp(-193 \rho_g^{-0.61} \mu_L^{0.5} \sigma_L^{0.11}) \quad (33)$$

- Liquid Axial Dispersion Coefficient

The liquid axial dispersion term is computed using the Deckwer's equation recommended by Shah et al. [25];

$$D_L = 0.68 D_c^{1.4} U_g^{0.33} \quad (34)$$

Similar values for  $D_L$  (m<sup>2</sup>/s) are gotten with the equation of Baird and Rice [26].

- Gas phase dispersion

Shah et al. [25] recommended the correlation of Mangartz and Pilhofer for calculating the gas phase dispersion term,  $D_g$ .

$$D_g = 50.0 D_c^{1.5} \left( \frac{U_g}{\varepsilon_g} \right)^3 \quad (35)$$

To approximate plug flow properties Peclet number for the large gas bubbles is set at 100 [21]. While, the small bubbles in the gas phase are assumed to have the same backmixing properties as the liquid [9, 28] so  $D_g$  is taken as equal to  $D_L$ .

## 2.4. Volumetric Mass Transfer Coefficient

The correlation of Akita and Yoshida recommended by Shah et al. [25] in their review as giving a fair estimate of the volumetric mass transfer term,  $k_L a$  is used for the UBM in this study.

$$\frac{k_L a D_c^2}{D_i} = 0.6 \left(\frac{v_L}{D_i}\right)^{0.5} \left(\frac{g D_c^2 \rho_L}{\sigma}\right)^{0.62} \left(\frac{g D_c^3}{v_L^2}\right)^{0.31} \times \varepsilon_g^{1.1} \quad (36)$$

Where  $D_i$  is the molecular diffusivity of solute in liquid phase ( $m^2/s$ ),  $v_L$  is the kinematic viscosity of liquid ( $m^2/s$ ) and  $\sigma$  is surface tension ( $N/m$ ).

For the LSBM,  $k_L a$  is determined using equations 37 and 38 for the distinct class of bubbles [16, 28]. This method of estimating  $k_L a$  was used by Boyer et al. [15] and Van der Laan et al. [20] in their works.

$$\frac{(k_L a)_{large}}{\varepsilon_b} = 0.5 \sqrt{\frac{D_i}{D_{i,ref}}} \quad (37)$$

$$\frac{(k_L a)_{small}}{\varepsilon_{df}} = 1.0 \sqrt{\frac{D_i}{D_{i,ref}}} \quad (38)$$

## 2.5. Rate Equation

The Yates and Satterfield [22] equation for cobalt catalyst (Co/MgO on SiO<sub>2</sub> support) is used in this study to represent the rate of reaction.

$$-r_{CO+H_2} = \frac{a P_{H_2} P_{CO}}{(1+b P_{CO})^2} \quad (39)$$

The term  $a$  in the equation above represents a kinetic parameter while  $b$  represents an adsorption coefficient. They are affected by temperature and are defined by the equations below derived by Maretto and Krishna [16] from curve-fitting of laboratory data.

$$a = 8.8533 \times 10^{-3} \exp \left[ 4494.41 \left( \frac{1}{493.15} - \frac{1}{T} \right) \right] \text{mols}^{-1} \text{kg}_{cat}^{-1} \text{bar}^{-2} \quad (40)$$

$$b = 2.226 \times \exp \left[ -8236 \left( \frac{1}{493.15} - \frac{1}{T} \right) \right] \text{bar}^{-1} \quad (41)$$

The rate at which the synthesis gas is being used up is expressed in terms of CO and H<sub>2</sub> by the relationship below (De Deugd, 2004):

$$-r_{CO+H_2} = -\frac{1}{v_{CO}} r_{CO} = -\frac{1}{v_{H_2}} r_{H_2} \quad (42)$$

$v_{CO}$  and  $v_{H_2}$  represents the stoichiometric coefficient of CO and H<sub>2</sub> respectively. With H<sub>2</sub>/CO equal to 2, the equation becomes;

$$-2r_{CO+H_2} = -2r_{CO} = -r_{H_2} \quad (43)$$

The rate model of Equation 39 is chosen since it is widely applied in literatures reviewed [9, 16, 28, 32] for the Fischer-Tropsch reaction using Co catalysts. The dimensionless form of the rate equation is as follows. Henry's law is used to relate partial pressures to liquid concentrations.

## 2.6. Physical Properties

The inlet gas consists of CO and H<sub>2</sub>. The inert liquid is paraffin wax mixture (reactor wax) having a mean number of 28 carbon atoms. Suspended in this complex liquid mix are solid catalyst particles loaded to concentrations as high as 0.35 (35 vol% slurry). The catalyst used is Co/MgO on SiO<sub>2</sub> support. The methods for determining density of the liquid, viscosity and surface tension are drawn from the works of Sehabiague [26] for 'reactor wax' and the Asymptotic Behaviour Correlation (ABC) given by Marano and Holder [33, 34]. The ABC model by Marano and Holder [33, 34] is popular in different literatures [7] for estimating the physical properties of the inert liquid. The diffusivity of the gas in the liquid can be approximated using the equations given by Erkey et al. [35]. The Erkey et al. [35] method is utilized in this study since it was specifically formulated for diffusivity in hydrocarbons (n-alkanes). The Henry's constant for the gas is calculated using the methods of Marano and Gormley [36]. The range of operating conditions investigated and some of the physical properties of the liquid and gas at 513K are presented in Table 1 and 2 respectively.

## 2.7 Resolution of Mathematical Model/Equations

The UBM (Equations 8 and 9) and LSBM equations (14, 15 and 16) and the attendant initial and boundary conditions are written for the reacting gases ( $H_2$  and  $CO$ ). The sets of equation are solved using MATLAB pdepe solver. An explanation of the technique implemented in the pdepe code for partial differential problems is given in the pdepe help files in MATLAB help.

**Table 1: Parametric Study Simulation Conditions**

Inlet $H_2/CO$ Ratio (Feed ratio)	1.0-2.5
Catalyst Volume Fraction	0.2-0.35
Superficial Gas Velocity m/s	0.1-0.40
Dispersion Height (m)	15-35
Reactor diameter (m)	8
Temperature (K)	513
Pressure (bar)	30

**Table 2: Physical Properties of Liquid and Gas (T=513K, P=30bar)**

Liquid Properties ( $C_{28}H_{58}$ )		Gas Properties		Solid (Catalyst) Properties (Krishna and Sie, 2000)
Liquid Density	$687 \text{ kg/m}^3$	Dimensionless Henry's constant, $m_{H_2}$	5.77	Cobalt/Magnesium Oxide supported on silica (21wt% Co and 3.9 wt% Mg)
Liquid Viscosity	$6.4 \times 10^{-4} \text{ Pa.s}$	Dimensionless Henry's constant, $m_{CO}$	4.64	Particle diameter = $50 \mu\text{m}$
Surface Tension	$1.7 \times 10^{-2} \text{ N/m}$	Diffusivity of $H_2$	$4.03 \times 10^{-8} \text{ m}^2/\text{s}$	Particle density = $647 \text{ kg/m}^3$
		Diffusivity of $CO$	$1.60 \times 10^{-8} \text{ m}^2/\text{s}$	

### 3. Results and Discussion

The concentration curves for hydrogen in the gas and liquid phases calculated using the UBM and LSBM are presented in Fig. 1(a, b). The estimates of the quantity of hydrogen converted are compared in Fig. 2. The UBM predicts higher hydrogen conversion than the LSBM throughout the length of reactor. However, both models predict almost similar conversion of hydrogen (88.2% and 87.2% respectively) at reactor outlet for the given reactor specifications and constraints. This observation follows closely that of Hooshyar et al. [23].

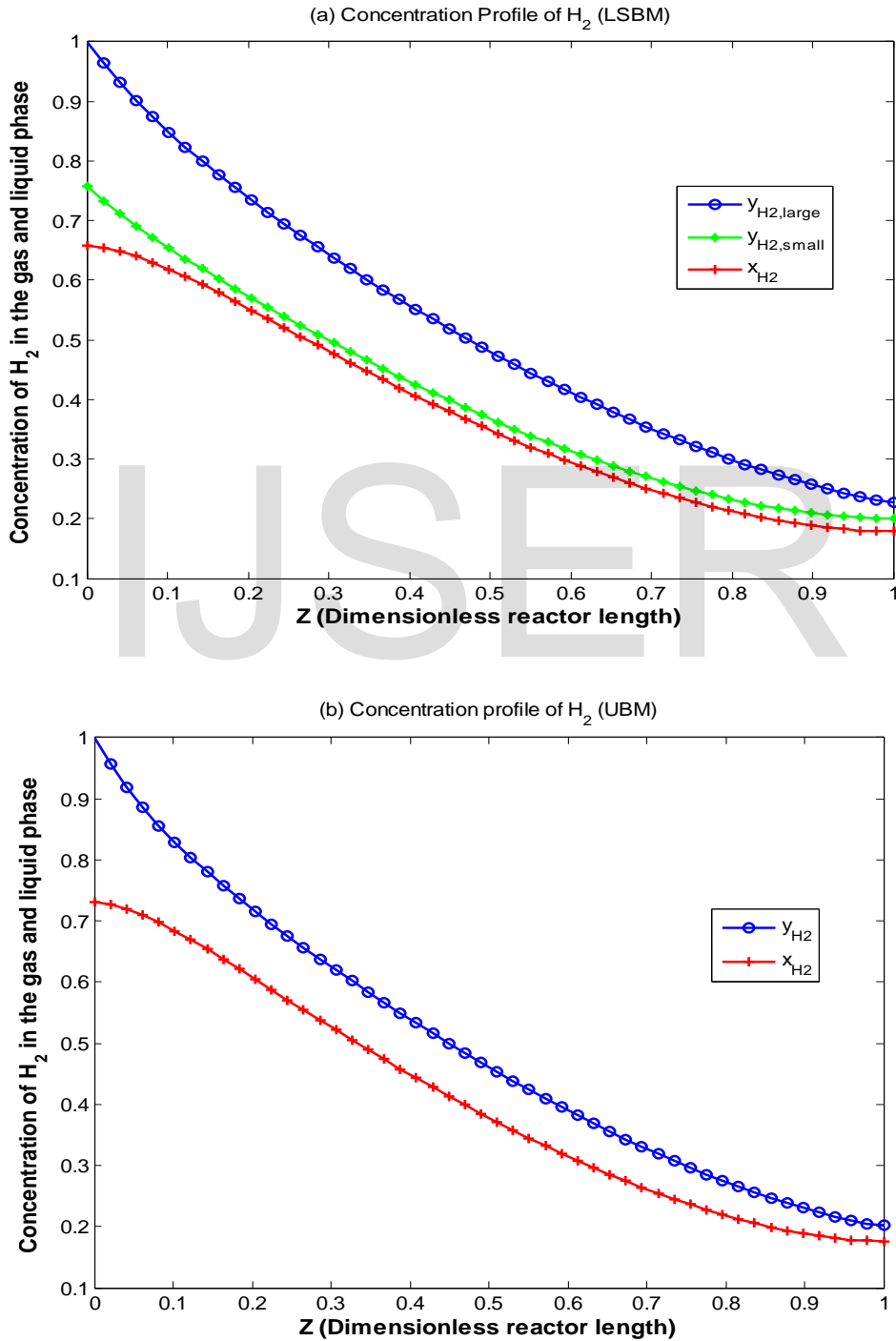


Figure 1: Concentration profile of Hydrogen. (a) LSBM (b) UBM ( $U_g=0.35$ ,  $\epsilon_s=0.35$ ,  $L=30m$ ,  $D_c=8m$ )



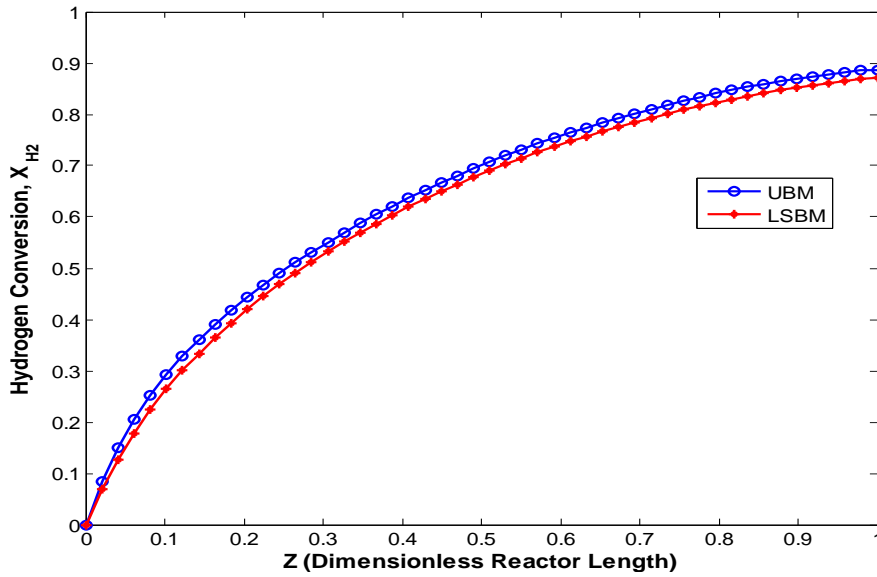


Figure 2: Comparison of Hydrogen Conversion profile of the UBM and LSBM Model

### 3.1 Comparison of Model Predictions at Different Catalyst Volume Fraction

The amount of hydrogen gas converted to products calculated using the UBM and LSBM at various catalyst holdups ( $\epsilon_s$  ranging from 0.2 to 0.4) is compared and illustrated in Fig. 3. It is noticed that with increasing holdup of catalysts, the distinction in gas conversion predictions become marginal. At catalyst loadings of 40% ( $\epsilon_s = 0.4$ ), the models predict similar hydrogen conversions of 92.1% (UBM) and 92.3% (LSBM).

This trend can be explained considering the fact that the gas holdup of the small bubbles reduces with higher catalyst holdup (or concentration). Several researchers [16, 28, 30] report that at high catalyst holdups ( $\epsilon_s > 0.38$ ) only large bubbles are present in the reactor as the small bubbles are ‘destroyed’. This implies that the distinction between the phases disappear leaving bubbles of almost uniform size, which may explain why the conversion values of the UBM and LSBM becomes closer with increasing catalyst holdup.

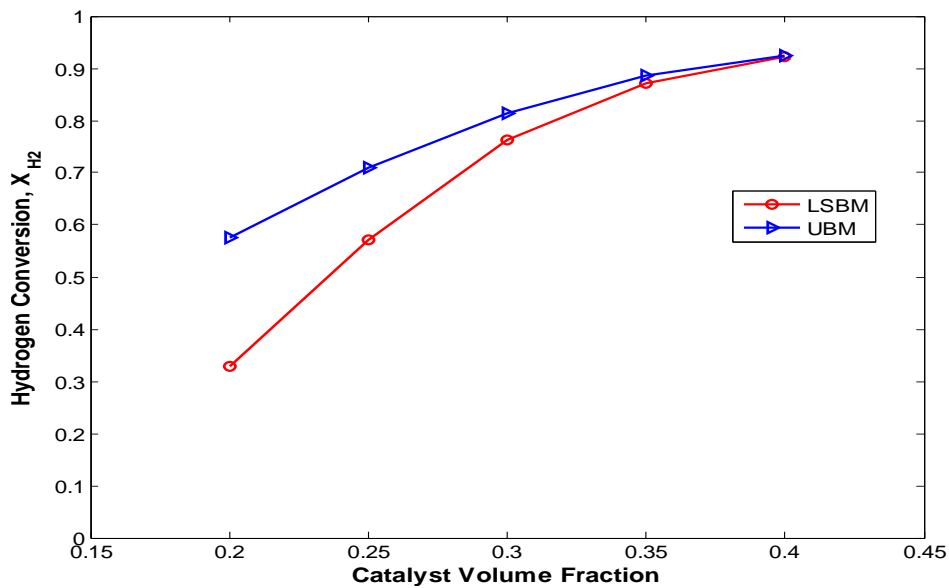


Figure 3: Comparison of Hydrogen Conversion at Different Catalyst Volume Fraction ( $U_g=0.35$ ,  $L=30m$ ,  $D_c=8m$ )

### 3.2 Comparison of Model Predictions using Different Gas Holdup Equations

The equations given by Maretto and Krishna [16] for calculating the small and large gas bubbles holdup and the total gas holdup are utilized in this work. The results for gas conversion at different inlet gas velocity and catalyst loadings are compared to values obtained when the gas holdup value of the small gas bubbles are determined from the correlations given by De Swart and Krishna [21] and Wilkinson [30].

A scrutiny of Fig. 4 (a, b, c) reveals that the choice of equations used in calculating the gas holdup can significantly affect the results obtained. It is observed that for every case simulated using different gas holdup correlations, the predictions for hydrogen conversion by the UBM were always higher than those of the LSBM. Both models also predict a decrease in hydrogen conversion as inlet gas velocity increases. When (Fig. 4a) the Maretto and Krishna [16] correlation is used for calculating the gas holdup, it is noticed that the difference in the hydrogen conversion values of the UBM and LSBM widens and becomes more pronounced at higher gas velocity for catalyst concentrations of 25% ( $\epsilon_s = 0.25$ ). At higher holdup of the catalyst ( $\epsilon_s = 0.35$ ), the variation in the predictions as the velocity of the inlet gas increases were more consistent and did not differ greatly. This observation is further corroborated when the findings obtained from analyzing Figure 4.4 is considered.

Analysis of Figs. 4b and 4c, where the De Swart and Krishna [21] and the Wilkinson's [30] methods are used respectively to compute the gas holdup of small bubbles showed little variation in model predictions at the lower and higher catalyst load with rising gas velocity when compared to Fig. 4a. The variation in the predictions and trend noticed when different gas holdup correlations are used suggests that the gas holdup equations play a key role in the ability of the models to accurately predict the performance of the reactor. It can be inferred that the difference in performance predictions of the UBM and LSBM may be connected to the correlation used in calculating the gas holdup. This observation brings to the fore the recommendation by Shah et al. [25] that it is better to estimate the gas holdup for a particular system from laboratory scale experiments.

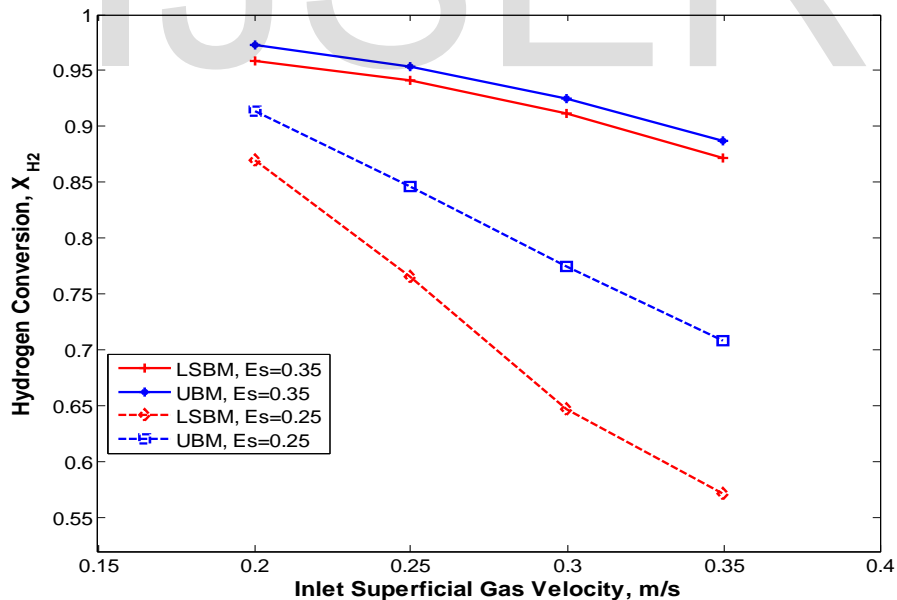


Figure 4(a): Hydrogen Conversion using Different Gas Holdup Correlations - Maretto and Krishna ( $L=30m$ ,  $D_c=8m$ )

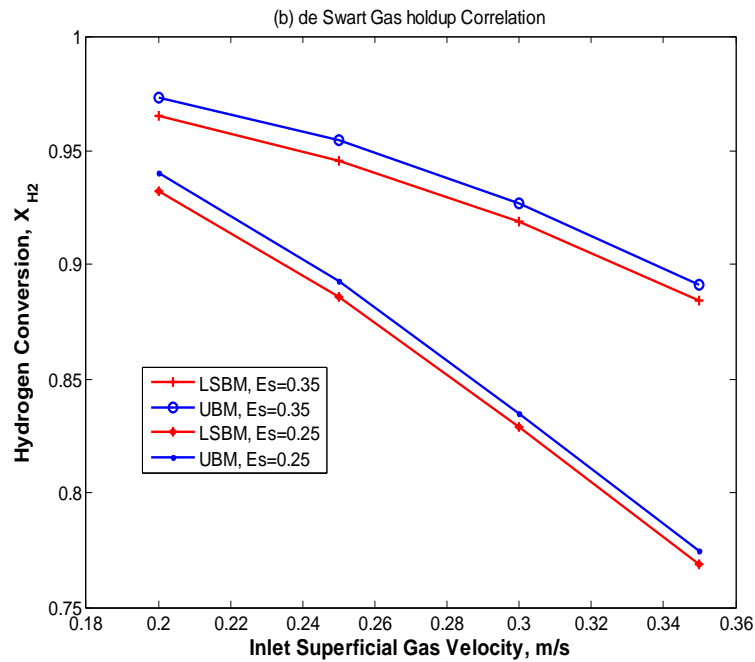


Figure 4(b): Hydrogen Conversion using Different Gas Holdup Correlations - De Swart ( $L=30m$ ,  $D_c=8m$ )

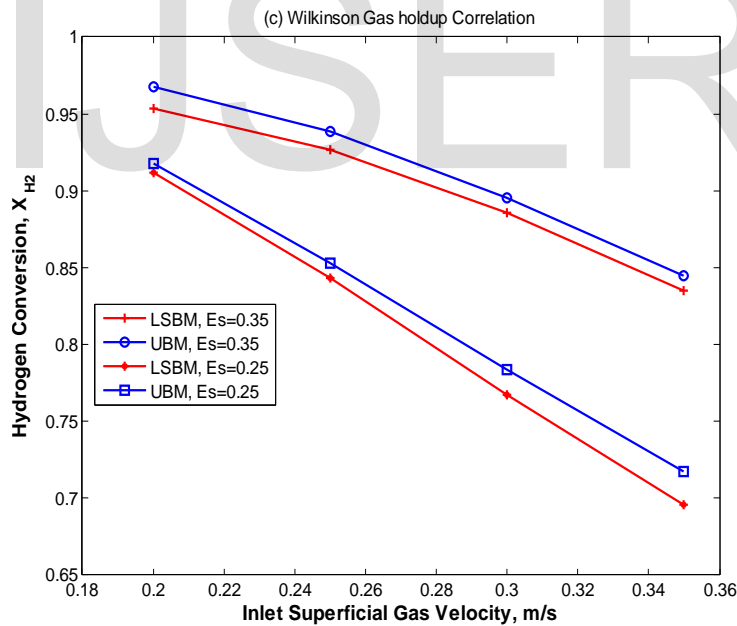


Figure 4(c): Hydrogen Conversion using Different Gas Holdup Correlations - Wilkinson ( $L=30m$ ,  $D_c=8m$ )

### 3.3 Comparison of Predictions for Different Gas Peclet number

The models are compared for predictions of hydrogen conversion when the Peclet number for the gas (UBM) and that of the large gas bubbles (LSBM) are set at different values. The results are shown in Table 3. The extent of backmixing of the phases described by the dispersion term affects the Peclet number. High gas dispersion coefficient gives low values of the Peclet number. Peclet number greater than 100 indicates small deviation from plug flow and vice versa. The UBM and LSBM estimates for gas conversion at different Peclet number are compared in Table 3.

Both models predict similar trend of increasing gas conversion with increased Peclet number (decreasing gas dispersion). The results indicate that increasing plug flow properties of the gas leads to higher conversion. At Peclet number above 100, very little difference is noticed in the reported values showing that setting the Peclet number at 100 adequately approximates plug flow properties for the gas phase (large bubbles in the LSBM). Wang et al. [37] who proposed an axial gas dispersion model using the penetration theory for gas-liquid systems reported trends similar to those observed in this work for Peclet number.

**Table 3: Comparison of Hydrogen Conversion at Different Peclet Numbers**

Peclet Number for Gas ( $Pe_g$ and $Pe_{g,large}$ )	Hydrogen Conversion (LSBM)	Hydrogen Conversion (UBM)
1	0.5026	0.5039
10	0.8191	0.8319
100	0.8715	0.8872
1000	0.8776	0.8941
10000	0.8782	0.8948

### 3.4 Effect of Reactor length

The impact of increasing the reactor length from 15m through 35m on hydrogen conversion is illustrated in Fig. 5. The conversion of hydrogen increases from 63.7% and 63.4% at the lower reactor length to 92.5% and 90.8% at reactor length of 35m for the UBM and LSBM respectively. There is only a slight difference in the values obtained by the models. However, it is noticed that this difference becomes more pronounced as the length of the reactor increases.

This rise in gas conversion when reactor length is increased was also reported by De Swart [31] and Sehabiague [26]. This improved conversion as the reactor gets taller can be explained with the longer time the gas spends in the reactor which allows for more reaction amongst the reacting gas.

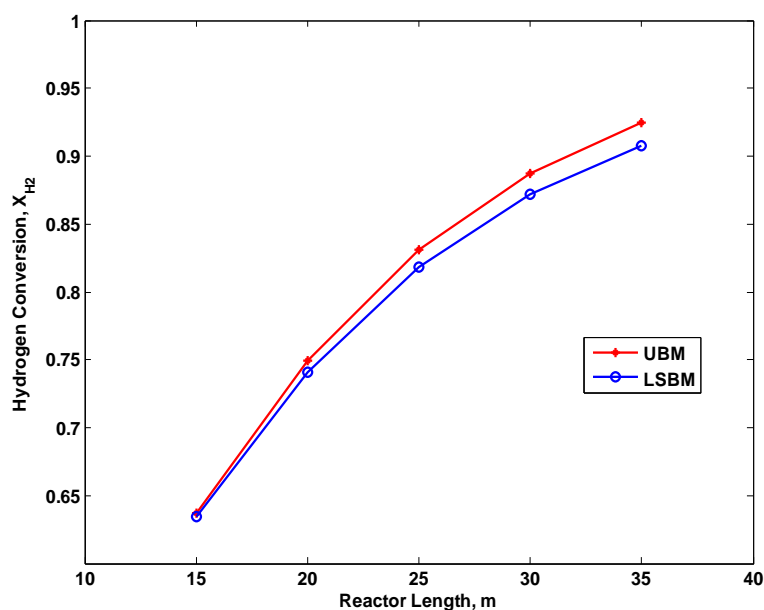


**Figure 5: Effect of Reactor Length on Hydrogen Conversion ( $U_g=0.35$ ,  $\epsilon_s=0.35$ ,  $D_c=8m$ )**

#### 4. Conclusion

Two mathematical models developed using the axial dispersion model for both the gas and liquid phases have been presented to study the Fischer-Tropsch synthesis in a Slurry Bubble Column Reactor. The predictions of the models for the conversion of hydrogen gas are compared. From the evaluation and comparison done, these conclusions are made:

- The UBM is as good a model as the LSBM for describing the performance of the reactor. Both models predict similar trend for gas concentration and conversion for the reactor constraints investigated
- The calculated amount of hydrogen gas conversion from simulations of the UBM were consistently higher than those of the LSBM for the cases considered
- At higher catalyst holdup ( $\epsilon_s > 0.35$ ) the distinction between the values for gas conversion calculated by the models narrows when the Marett and Krishna [16] equation for gas holdup is used
- The difference and accuracy in the values of the UBM and LSBM may as well be related to the correlations or method used in calculating the gas holdup values. This emphasizes the importance of hydrodynamic parameters such as gas holdup in the design and scale-up of slurry bubble reactors. It is imperative that gas holdup values describe the behaviour of the system as closely as possible
- Increasing the velocity of the inlet gas decreases the conversion of gas while loading more catalyst into the reactor and increasing the length of the reactor increases conversion. It is recommended that the reactor should be operated at moderate gas velocity and catalyst loads to maximize conversion

#### LIST OF SYMBOLS

$a$	Gas-liquid interfacial area per unit liquid, $m^{-1}$
$a$	Kinetic parameter in the Yates and Satterfield rate equation, $mols^{-1}kg_{cat}^{-1}bar^{-2}$
$A_C$	Cross sectional area, $m$
$b$	Adsorption coefficient in the Yates and Satterfield rate equation, $bar^{-1}$
$C_{A,g}$	Concentration of species A in the gas phase, $mol/m^3$
$C_{A,L}$	Concentration of species A in the liquid phase, $mol/m^3$
$C_{Ai}$	Concentration of species A at liquid interphase, $mol/m^3$
$C_{Ao}$	Inlet concentration of specie A in the gas phase, $mol/m^3$
$D_{AB}$	Diffusivity of gas A in liquid B, $m^2/s$
$D_c$	Diameter of column, $m$
$D_g$	Gas axial dispersion parameter, $m^2/s$
$D_L$	Liquid axial dispersion parameter, $m^2/s$
$D_i$	Molecular diffusivity of solute in liquid phase, $m^2/s$
$d_{vs}$	Sauter mean bubble diameter, $m$
$F$	Feed/Inlet gas ratio, $H_2/CO$
$F_A$	Molar flowrate of component A, $mol/s$
$g$	Acceleration due to gravity, $m/s^2$
$H_A$	Henry's constant, $bar\,m^3/mol$
$k_g a$	Volumetric gas side mass transfer coefficient, $s^{-1}$
$k_L$	Mass transfer coefficient, $m/s$
$k_L a$	Liquid side volumetric mass transfer coefficient, $s^{-1}$
$K_L a$	Overall volumetric mass transfer coefficient, $s^{-1}$
$L$	Length of reactor, $m$
$m_A$	Dimensionless Henry's constant
$P_A$	Partial pressure of component A, $bar$
$P_{Ai}$	Partial pressure at gas-liquid interphase, $bar$
$Pe_g$	Peclet number of the gas, dimensionless
$Pe_{g,large}$	Peclet number of the large gas, dimensionless
$Pe_{g,small}$	Peclet number of the small gas, dimensionless

$Pe_L$	Peclet number of the liquid, dimensionless
$P_T$	Total pressure, <i>bar</i>
$-r_A$	Intrinsic rate of reaction, <i>mol/kg<sub>cat</sub>.s</i>
$Sh$	Sherwood number, dimensionless
$St_g$	Stanton number of the gas phase, dimensionless
$St_L$	Stanton number of liquid phase, dimensionless
$t$	Time, <i>s</i>
$T$	Temperature, <i>K</i>
$U$	Consumption ratio, $(-r_{H_2}/-r_{CO})$
$U_B$	Superficial gas velocity through the large bubbles, <i>m/s</i>
$U_{df}$	Superficial gas velocity through the small bubbles, <i>m/s</i>
$U_g$	Superficial gas velocity, <i>m/s</i>
$U_{go}$	Inlet superficial gas velocity, <i>m/s</i>
$U_L$	Superficial liquid velocity, <i>m/s</i>
$U_{trans}$	Gas velocity at transition point, <i>m/s</i>
$V$	Volume, <i>m<sup>3</sup></i>
$V_L(0)$	Centerline liquid velocity, <i>m/s</i>
$V_{small}$	Rise velocity of small bubbles, <i>m/s</i>
$x_A$	Concentration of specie A in the liquid, dimensionless
$X_A$	Conversion of Species A
$X_{CO+H_2}$	Syngas conversion
$y_A$	Dimensionless concentration of specie A
$y_{Ao}$	Initial concentration of specie A, dimensionless
$Z$	Dimensionless length of reactor
$z$	Length of element, <i>m</i>

### Greek Symbols

$\epsilon_b$	Large bubble holdup
$\epsilon_{df}$	Small bubble holdup
$\epsilon_{df,ref}$	Reference value of gas holdup of small bubbles
$\epsilon_g$	Gas holdup
$\epsilon_L$	Liquid holdup
$\epsilon_S$	Solids holdup
$\mu_{eff}$	Effective viscosity, <i>pa.s</i>
$\mu_L$	Viscosity of liquid, <i>pa.s</i>
$\nu_L$	Kinematic viscosity of liquid, <i>m<sup>2</sup>/s</i>
$\rho_g$	Gas density, <i>kg/m<sup>3</sup></i>
$\rho_L$	Liquid density, <i>kg/m<sup>3</sup></i>
$\rho_S$	Solids density, <i>kg/m<sup>3</sup></i>
$\rho_{sl}$	Slurry density, <i>kg/m<sup>3</sup></i>
$\tau$	Dimensionless time
$\sigma$	Surface Tension, <i>N/m</i>

### REFERENCES

1. Jager, B., Development of Fischer Tropsch Reactors. *Paper presented at the AIChE Spring meeting*, New Orleans, 1 April, 2003.
2. Xiuli, W. and Economides, M., *Advanced natural gas engineering* (Gulf Publishing Company, Houston Texas, 2009)
3. Khan W.A., Shamshad I., Shafiq U. and Mukhtar A., Design methodology for the Fischer-Tropsch reactor for the production of green diesel from coal syngas. *European Journal of Advances in Engineering and Technology* 2(9), 2015, 20-24
4. Fajin, J.L.C., Cordeiro, N.D.S., Gomes, J.R.B., Fischer Tropsch Synthesis on Multicomponent Catalysts: What can we learn from computer simulations? *Catalysts Vol 5*, 2015, 3-17

5. Elbashir, N.O, Bao, B. and El-Halwagi, M.M., An approach to the design of advanced Fischer-Tropsch reactor for operation in near-critical and supercritical phase media. *Proceedings of the 1<sup>st</sup> Annual Gas Processing Symposium*, 2009
6. Nafees, A. and Al-Hashimi, S.H., Fischer-Tropsch Gas to Liquid Technology (GTL). *The Second International Energy 2030 Conference*, Abu Dhabi, U.A.E, November 4-5, 2008
7. Van der Laan, G.P., *Kinetics, selectivity and scale up of the Fischer Tropsch synthesis*, PhD Thesis, University of Groningen, The Netherlands, 1999
8. Prakash, A. and Bendale, P.G., Design of Slurry Reactor for Indirect Liquefaction Applications. *Paper presented at U.S. DOE Indirect Liquefaction Contractor's Review Meeting*, Pittsburg, Pennsylvania. November 6-8, 1990
9. Schabiague, L., Lemoine, R., Behkish, A., Heintz, Y.T., Mareila, S., Onkaci, R. and Morsi, B.I., Modeling and optimization of a large scale slurry bubble column reactor for producing 10,000 bbl/day of Fischer-Tropsch liquid hydrocarbons. *Journal of Chinese Institute of Chemical Engineers*, Vol 39, 2008, 169-179
10. Bukur, D.B., Daly, J.G., Patel, S.A., Raphael, M.L. and Tatterson, G.B., Hydrodynamics of Fischer-Tropsch Synthesis in Slurry Bubble Column Reactors. *Final report prepared for United States Department of Energy under Contract No. DE-AC22-84PC70027*, 1987
11. Forret, A., Schweitzer, J.M., Gauthier, T., Krishna, R. and Schweich, D., Scale up of Slurry Bubble Reactors. *Oil & Gas Science and Technology*, Vol 61, No. 3, 2006, 443-458
12. Inga, J.R., *Hydrodynamic studies and reactor modeling of a three phase slurry reactor in Fischer Tropsch applications*. Master Thesis. Potchefstroom University for Christian Higher Education, 1992
13. Guettel, R. and Turek, T., Comparison of Different Reactor Types for Low Temperature Fischer-Tropsch Synthesis: A simulation study. *Journal of Chemical Engineering Science*, vol 64, 2009, 955-964
14. Schweitzer, J.M. and Viguie, J.C. (2009): Reactor Modeling of a Slurry bubble Column for Fischer-Tropsch Synthesis. *Oil & Gas Science and Technology*, Vol 64, No. 1, 2009, 63-77
15. Boyer, C., Gazarian, J., Lecocq, V., Maury, S., Forret, A., Schweitzer, J.M., Souchon, V., Development of the Fischer-Tropsch Process: From the Reaction Concept to the Process Book. *Oil & Gas Science and Technology – Rev IFP Energies nouvelles*, Vol 71, 44, 2016
16. Maretto, C. and Krishna, R., Modeling of a bubble column slurry reactor for Fischer-Tropsch synthesis. *Catalysis Today*, Vol 52, 1999, 279-289
17. Rados, N., Al-Dahhan, M.H., Dudukovic, M.P., Modeling of the Fischer-Tropsch Synthesis in Slurry Bubble column Reactors. *Catalyst today*, 79-80, 2003, 211-218
18. Wang, Y., Wei, F., Ying L., Zeng, Z., Hao, X., Chang, M., Zhang, C., Xu, Y., Xiang, H. and Li, Y., Modeling of the Fischer-Tropsch Synthesis in Slurry Bubble Column Reactors. *Chemical Engineering and Processing*, Vol 47, 2008, 222-228
19. Iliuta, I., Larachi, F., Anfray, J., Dromard, N. and Schweich, D., Multicomponent Multicompartment Model for Fischer-Tropsch SBCR. *AIChE Journal*, Vol. 53(8), 2007, 2026-2083
20. Van der Laan, G.P., Beenackers, A.A.C.M. and Krishna, R., Multicomponent reaction engineering model for Fe-catalyzed Fischer-Tropsch synthesis in commercial scale slurry bubble column reactors. *Chemical Engineering Science* 54, 1999, 5013-5019
21. De Swart, J.W.A. and Krishna, R., Simulation of the transient and steady state behavior of a bubble column slurry reactor for Fischer Tropsch synthesis. *Chemical Engineering and Processing* 41, 2002, 35-47
22. Yates, I.C. and Satterfield, C.N., Intrinsic kinetics of the Fischer-Tropsch synthesis on a cobalt catalyst. *Energy fuels*, Vol 5, 1991, 168-173
23. Hooshyar, N., Fatemi, S., Mohammad, R., Mathematical Modeling of Fischer-Tropsch in Industrial slurry Bubble column. *International Journal of Chemical Reactor Engineering*, Vol. 7, Article A23, 2009
24. Papari, S., Kazemini, M. and Fattahi, M., Mathematical Modeling of a Slurry Reactor for DME Direct Synthesis from Syngas. *Journal of Natural Gas Chemistry*, Vol 21, 2012, 148-157
25. Shah, Y.T., Kelkar, B.G., Godbole, S.P. and Deckwer, W.D., *Design Parameters Estimations for Bubble Column Reactors*. *AIChE Journal*, Vol 28(3), 1982, 353-379
26. Schabiague, L., *Modeling, Scale up and Optimization of Slurry Bubble Column Reactors for Fischer-Tropsch synthesis*. PhD project submitted to the Graduate Faculty of Swanson School of Engineering, University of Pittsburg, 2012
27. Fox, J.M., Degen, B.D., Cady, G., Deslate, F.D., Summers, R.L., Akgerman, A. and Smith, J.M. (1990): *Slurry Reactor Design Studies*. United States: N.p. web.doi:10.2172/6094135
28. Krishna, R. and Sie, S.T., Design and scale up of the Fischer-Tropsch bubble column slurry reactor. *Fuel Technology*, Vol 64, 2000, 73-105
29. Krishna, R., van Baten, J.M., Urseanu, M.I., Ellenberger J., Design and scale up of a bubble column slurry reactor for Fischer-Tropsch synthesis. *Chemical Engineering Science*, Vol 56, 2001, 537-545

30. Behkish, A., *Hydrodynamic and Mass Transfer Parameters in Large scale Slurry Bubble Column Reactors*. PhD thesis, University of Pittsburg, 2004
31. De Swart, J.W.A., *Scale up of a Fischer-Tropsch Slurry Reactor*. PhD Thesis University of Amsterdam, Amsterdam, Netherlands, 1996
32. Kim, Y.H., Jun, K., Joo, H., Han, C. and Song, I.K., A simulation study on gas-to-liquid (natural gas to Fischer-Tropsch synthetic fuel) process optimization. *Chemical Engineering Journal*, Vol 144, 2009, 427-432
33. Marano, J. and Holder, G.D., General Equations for Correlating the Thermophysical Properties of n-Paraffins, n-Olefins, and other Homologous Series. 1. Formalism for Developing Asymptotic Behavior Correlations. *Ind. Eng. Chem Res.* 36,1997, 1887-1894
34. Marano, J. and Holder, G.D., Prediction of Bulk Properties of Fischer-Tropsch Derived Liquids. *Ind. Eng. Chem. Res.* 36, 1997 2409-2420.
35. Erkey, C., Rodden, J.B., Agkerman, A., A correlation for predicting diffusion coefficients in Alkanes. *The Canadian Journal of Chemical Engineering*, Vol 68, 1990
36. Marano, J.J. and Gormley, R.J., *Effects of slurry composition on the reaction of the Fischer-Tropsch synthesis*, [www.lorentzcenter.nl/lc/web/2012/512/problems](http://www.lorentzcenter.nl/lc/web/2012/512/problems)
37. Wang, J., Han, S., Wei, F., Yu, Z. and Jin, Y., An axial dispersion model for gas-liquid reactors based on the penetration theory. *Chemical Engineering and Processing*, 36,1997, 291-299

# IJSER